

Characterization of Thermoplastic Composites Developed with Wheat Straw and Enzymatic-hydrolysis Lignin

Chunhan Yu,^{a,b,Φ} Wentao Zhang,^{a,b,Φ} Lemma Dadi Bekele,^a Xiang'an Lu,^a Gregory Joseph Duns,^{a,c} Leilei Jin,^a Qi Jia,^b and Jishuang Chen^{a,b,*}

Novel thermoplastic composites filled with wheat straw (WS) and enzymatic-hydrolysis lignin (EHL) were developed and characterized. The three-dimensional melt blending system of WS, EHL, and high-density polyethylene (HDPE) was optimized *via* orthogonal experiments. The mechanical properties and melt index of the composites were measured and the optimum ratio of the composites was determined. Based on the optimum ratio of the composites' blending system, identified through compounding granulation and extrusion molding process links, pilot products of the composites were produced. The thermal behavior, polar groups, and surface structures of the fibers and developed thermoplastic composites were assessed by thermogravimetric analysis (TGA), Fourier transform infrared spectroscopy (FT-IR), and scanning electron microscopy (SEM) analysis, respectively. The addition of EHL, an abundant renewable resource, improved the dispersity of the matrix as well as the mechanical and thermal properties of the composites. The results provide a theoretical basis for the application and development of new composites and illustrate a potential industrial application of EHL.

Keywords: Wheat straw; Enzymatic-hydrolysis lignin; Polyethylene; Composites; Characterization

Contact information: a: College of Biotechnology and Pharmaceutical Engineering, Nanjing Tech University, Nanjing, 211800, Jiangsu, China; b: Zunyi Medical University, Zunyi, 563000, Guizhou, China; c: AirChem Consulting and Research, London, Ontario, Canada; Φ: These authors contributed to the work equally and should be regarded as co-first authors;

* Corresponding author: biochenjs@njtech.edu.cn

INTRODUCTION

In recent years, as biomass resources have been developed, the utilization of straw biomass has received increasing attention. Straw fiber is an important bioresource in China, and making full use of straw is an effective way to exploit what would otherwise be a source of environmental pollution. Straw fiber is an important renewable biomass resource that has a high strength and modulus (Selke and Wichman 2004). Therefore, studies on straw biomass and its application in polymer matrix composites have attracted much attention from both the scientific community and industries (Panthapulakkal *et al.* 2006; Han *et al.* 2010; Zou *et al.* 2010). Still, the performance of straw biomass in composites is influenced by the natural characteristics of straw, such as susceptibility to mold attack and hence poor resistance to aging in the resulting composites (Rangaraj and Smith 2000; Matuana and Stark 2003; Wang *et al.* 2008).

Enzymatic-hydrolysis lignin (EHL) is a by-product of biofuel ethanol production with lignocellulosic materials. The decomposition of cellulose and hemicellulose in straw and other agricultural by-products occurs *via* biological enzymes when they are used as

raw materials for the production of bioethanol. Enzymatic hydrolysis lignin is the product obtained by the separation and purification of the degradation residue (Xiao *et al.* 2001; Kosikova and Gregorova 2005). Today, enzymatic-hydrolysis lignin residues are usually burned as fuel to generate power in pulping industry. This way of treatment not only has low economic benefit, but it also can easily cause certain pollution to the environment. The application of lignin in polymeric materials not only can help make full use of renewable resources, but it also reduces the pollution caused by the synthesis of polymer materials in the pulp and paper industry. Therefore, thermoplastic composites developed with enzymatic-hydrolysis lignin represent a viable solution with potential economic and environmental benefits. Recently, there has been research on enzymatic hydrolysis lignin and plastic, rubber, and other polymer materials to form composite materials with enhanced mechanical properties (Rodrigues *et al.* 2002; Alexy *et al.* 2004; Cazacu *et al.* 2004; Feldman *et al.* 2007). Pucciariello *et al.* (2004) introduced EHL to linear low density polyethylene (LLDPE) and low density polyethylene (LDPE) materials to prepare composites. The results showed that the mechanical properties of the composites with lignin were reduced, but the addition of lignin increased the anti-ultraviolet (UV) aging performance of the composites, suggesting that lignin has the potential to act as an antioxidant stabilizer in plastics.

The authors have previously studied the mechanical properties of modified wheat straw/high-density polyethylene (MWS/HDPE) straw-plastic composites, and it has been shown that the use of CaCO₃ as a modifying component improves the mechanical performance of the resulting composite (Zhang *et al.* 2016). Additionally, other studies have been conducted on the application of straw fiber raw materials in thermoplastic composites. These studies mainly focused on the composite interface and preparation process, specifically, the influences of single plant fiber on polypropylene matrix or polyethylene matrix composites properties. (Gregorová *et al.* 2005; Canetti *et al.* 2006; Liany *et al.* 2013). However, the literature available on the application of multiple fibers from different sources and polyethylene blends in composite materials is insufficient. In particular, there have been no reports on using WS/EHL and polyethylene to form a three-dimensional blending system composite material. Therefore, it is necessary to further investigate the aforementioned natural fiber type and processing technology through the interplay of different biomass characteristics and attempt to optimize the overall performance of composites. Moreover, the use of various reinforcement in the polymer matrices are usually hindered because of the lack of compatibility between the hydrophilic natural fibers components and hydrophobic polymer matrices (Wambua *et al.* 2003; Maneesh *et al.* 2012). Use of chemical coupling agents in composite processing has been reported as the best way to achieve enhanced compatibility between the components (Toress and Cubillas 2005; Sirapat *et al.* 2012; Bekele *et al.* 2017). Mengeloglu *et al.* (2007) reported that the use of maleated polypropylene (MAH-g-PP) coupling agent can significantly increase the tensile strength and tensile modulus of both HDPE-WFC and PP-WFC composite. Furthermore, it has been shown that the MAH-g-PP coupling agent slightly increased the flexural strength of HDPE-WFC. In this study, thermoplastic composites of WS/EHL and polyethylene were prepared under the three-dimensional melt blending system to identify the optimal proportion of the raw materials for preparing the composites. The thermal stability, chemical structure, and microstructure of the composites were also investigated.

EXPERIMENTAL

Materials

Wheat straw (WS) was collected in March 2016 from Zhoukou in the Henan Province in China. After natural drying, it was dried at 80 °C for 5 h and then ground in a pulverizer to obtain straw fibers (40 to 60 mesh particle size). The EHL was supplied by the National Biochemical Engineering Technology Research Center of Nanjing University of Technology (100 mesh particle size, Nanjing, China). High-density polyethylene (HDPE, 9001, melt flow index of 3.24 g/10 min, density of 0.965 g/cm³, and melting point of 135 °C), used as the polymer matrix, was obtained from the Sinopec Group of Nanjing, China. Calcium carbonate (CaCO₃) of 800-mesh particle size was obtained from Shunxin Calcium Carbonate Co., Ltd. of Xuancheng, China. The maleic anhydride grafted polypropylene (MAH-g-PP) and potassium bromide used were provided by Nanjing Jufeng Advanced Materials Co., Ltd., of Jiangsu Province, China.

Orthogonal Experimental Design

The contents of WS, EHL, CaCO₃, and MAH-g-PP were selected as the experimental factors, and the mechanical properties and melt index of composite materials (MFR) were used as indices. The experiment was designed according to orthogonal tables of four factors and three levels. All the factors and levels are shown in Table 1. Various factors were added to the scheme relative to the quality content of the matrix polyethylene (HDPE). The orthogonal experimental design and the various factors of the matching scheme are shown in Table 2. Statistical analysis of orthogonal experimental design was performed using SPSS software (IBM, version 25.0, Chicago, IL, USA).

Table 1. The Factors of Levels by Orthogonal Experiments

Factor Level	[A] WS (%)	[B] EHL (%)	[C] CaCO ₃ (%)	[D] MAH-g-PP (%)
1	30	5	5	1
2	40	15	10	3
3	50	30	20	5

Table 2. Experimental Design of Orthogonal Tests

Factor Group	[A] WS (%)	[B] EHL (%)	[C] CaCO ₃ (%)	[D] MAH-g-PP (%)
1	(A1) 30	(B1) 5	(C1) 5	(D1) 1
2	(A1) 30	(B2) 15	(C2) 10	(D2) 3
3	(A1) 30	(B3) 30	(C3) 20	(D3) 5
4	(A2) 40	(B1) 5	(C2) 10	(D3) 5
5	(A2) 40	(B2) 15	(C3) 20	(D1) 1
6	(A2) 40	(B3) 30	(C1) 5	(D2) 3
7	(A3) 50	(B1) 5	(C3) 20	(D2) 3
8	(A3) 50	(B2) 15	(C1) 5	(D3) 5
9	(A3) 50	(B3) 30	(C2) 10	(D1) 1

Processing of Composites

The WS fibers, EHL, CaCO₃, and other experimental materials were placed in a constant temperature drying oven at 80 °C for 24 h and dried to a moisture content of below

5%. Then, according to the orthogonal experimental design, the raw materials of the nine groups were weighed and melt blended into composites using a two-spindled mechanical mixer (Suyan Science and Technology Corporation, Nanjing, China) at a temperature of 180 °C for 6 min. After mixing, the specimens were compressed into composite panels using an SLB-25-D350 Carver hydraulic hot press molding machine (Suyan Science and Technology Corporation, Nanjing, China) at 190 °C for 20 min under a loading of 5 MPa. The composites were then stored at room temperature conditions for 24 h before their use in mechanical and physical tests.

Methods

Testing of mechanical properties

The flexural and tensile properties were determined using a UTM-1422 standard electronic universal testing machine (Jinjian Testing Instrument Corporation, Chengde, China). The flexural properties were measured in accordance with ASTM D790 (2010). The test conditions were as follows: the loading speed was 2 mm/min and the span was 16 times the thickness of the sample. The tensile properties were determined according to the ASTM D638 (2010) standard, using the aforementioned testing machine. The test conditions were as follows: the drawing speed was 50 mm/min and the line spacing was 50 mm. The ASTM D256 (2010) method was used for the series of Izod impact tests conducted using a XJUD-5.5 pendulum type impact machine (Jinjian Testing Instrument Corporation, Chengde, China). All of the mechanical properties tests were performed at room temperature and five measurements were made for each composite.

The flexural and compressive properties of the composite pilot products were tested by ASTM D6109 (2010). The sample size was $L = (16h + 50) \text{ mm} + 2 \text{ mm}$, in which “ h ” is the thickness of the sample, the span is 16 times the sample thickness, and the loading speed is 2 mm/min. The selected test scheme and raw materials were passed through granulation, extrusion, and other process steps to ultimately obtain the products.

Determination of melt index of composites

The composites were prepared into particles with a diameter of approximately 2 mm, and their melt index was measured by a mass method with a melt flow rate meter (Jinjian Testing Instrument Corporation, Chengde, China) in accordance with the method prescribed by the ASTM D1238 standard (2013). The tests were performed at a temperature of 190 °C and a load of 2.16 kg. All results were taken as the average value of three different specimens.

Thermogravimetric analysis

Thermogravimetric analysis of the material was measured using a Netzsch STA 449C synchronous thermal analyzer (Netzsch, Bavaria, Germany). The thermal decomposition of the composites was measured with a continuous heating procedure. The test was conducted by heating the specimens from 35 °C to 600 °C at a rate of 10 °C/min in an atmosphere of nitrogen (N₂), and the gas flow rate was 30 mL/min.

Fourier transform infrared measurements

The composite material was analyzed by FT-IR spectrometry (Thermo Electron Corporation, Massachusetts, USA). The test material was dried at 80 °C for 5 h, and the dried specimen was placed in a mortar, mixed with 300 mg potassium bromide (KBr) powder, and was finely ground and homogeneously blended. A 200 mg quantity of the

homogenously mixed sample powder was taken and compression casted into a thin sheet at 20 MPa for 3 min. The infrared spectrum scanning conditions included a resolution of 440 cm^{-1} to 4000 cm^{-1} and a scan rate of 40/min.

Scanning electron microscopy

The samples were placed in liquid nitrogen for 10 min and then broken along their long axis to obtain a fractured surface. The fractured composites were then mounted on a plate with black sticky tape and gold sputtered (Leica, Wetzlar, Germany) prior to microscopic analysis using a scanning electron microscope (TM-3000 Hitachi, Tokyo, Japan).

RESULTS AND DISCUSSION

Orthogonal Experiment Results Determining the Optimal Proportion of Composite Materials

The contents of WS, EHL, CaCO_3 , and MAH-g-PP were taken as experimental factors to design orthogonal experiments with four factors and three levels L_9 (3^4). The flexural strength, tensile strength, impact strength, and melt index of the composites were investigated to determine the optimal ratio of the composites *via* comprehensive equilibrium analysis (Deng and Zhao 2016). Orthogonal test results are shown in Table 3.

Table 3. The Results of Orthogonal Experiments of Different Composites

Index Group	Flexural Strength (MPa)	Tensile Strength (MPa)	Impact Strength (KJ/m ²)	Melt Index (g/10 min)
1	28.79	16.83	3.67	1.56
2	31.15	18.02	3.64	1.28
3	29.25	16.78	2.98	0.69
4	28.74	19.57	3.28	1.20
5	29.72	13.98	3.28	0.84
6	28.21	14.55	2.99	1.66
7	38.94	18.69	3.58	0.79
8	37.06	18.02	3.41	0.95
9	30.60	14.51	3.47	0.49

Analysis of Mechanical Properties of Different Composites

The results of the mechanical properties tests of the different composites, tested using orthogonal experiments, are shown in Tables 4 through 6.

Table 4. Flexural Strength Test for Different Composites

Factor Level	[A] WS (%)	[B] EHL (%)	[C] CaCO_3 (%)	[D] MAH-g-PP (%)
*K ₁	89.19	96.47	94.06	89.11
K ₂	86.67	97.93	90.49	98.30
K ₃	106.60	88.06	97.91	95.05
**R	6.64	3.29	2.48	3.07

Note: *K₁ represents the sum of the test results corresponding to the level number 1 on any column; and **R represents the extreme value.

Table 5. Tensile Strength Test for Different Composites

Factor Level	[A] WS (%)	[B] EHL (%)	[C] CaCO ₃ (%)	[D] MAH-g-P (%)
K ₁	51.63	55.09	49.40	45.32
K ₂	48.10	50.02	52.10	51.26
K ₃	51.22	45.84	49.45	54.37
R	1.18	3.08	0.90	3.01

Table 6. Impact Strength Test for Different Composites

Factor Level	[A] WS (%)	[B] EHL (%)	[C] CaCO ₃ (%)	[D] MAH-g-PP (%)
K ₁	10.29	10.53	10.07	10.42
K ₂	9.55	10.33	10.39	10.21
K ₃	10.46	9.44	9.84	9.67
R	0.31	0.36	0.18	0.25

The range according to the size of the sequence was $R_A > R_B > R_D > R_C$, so the order of the factors that influenced the flexural strength of the material was $A > B > D > C$, as shown in Table 4. According to the analysis of the flexural strength test results, the optimized formula was $A_3B_2C_3D_2$. Similarly, as shown in Tables 5 and 6, the optimum formula for tensile properties was $A_1B_1C_2D_3$, and the formula for optimum impact strength was $A_3B_1C_2D_1$.

Analysis of the Melt Index

The melt index range according to the size of the sequence was $R_C > R_A > R_D > R_B$, as shown in Table 7. Therefore, the order of the factors that influenced the melt index of the material was $C > A > D > B$. According to the melt index test results, the optimized formula was $A_2B_1C_1D_2$. Thus, the optimized filling amount was 40% for WS, 5% for EHL, 5% for CaCO₃, and 3% for MAH-g-PP.

Table 7. The Melt Index Test for Different Composites

Factor Level	[A] WS (%)	[B] EHL (%)	[C] CaCO ₃ (%)	[D] MAH-g-PP (%)
K ₁	3.53	3.55	4.17	2.89
K ₂	3.70	3.07	2.97	3.73
K ₃	2.23	2.84	2.32	2.84
R	0.49	0.23	0.62	0.29

Determination of Optimal Matching Conditions

Based on the results above, several factors, including the flexural strength, tensile strength, impact strength, and melt index were not consistent among all tests. Thus, it was necessary to consider the optimal order of these four indices and determine the optimal matching conditions.

Identified by comprehensive balance analysis, the optimal conditions of this experiment were $A_3B_1C_1D_3$. Therefore, the optimal filling amount was 50% for WS, the amount of lignin (EHL) was 5%, the CaCO₃ content was 5%, and the content of MAH-g-PP was 5%. This particular set of conditions was not included in the 9 groups of tests;

accordingly the results of the experiments to verify the optimal matching conditions are shown in Table 8.

Table 8. Verification of Results Under the Optimal Matching Conditions

Parameter Index	Numerical Value
Flexural strength (MPa)	42.22
Tensile strength (MPa)	19.89
Impact strength (KJ/m ²)	4.12
Melt index (g/10 min)	2.07

The flexural strength, tensile strength, and impact strength of the composites prepared by the optimum ratio were 42.2 MPa, 19.9 MPa, and 4.12 KJ/m², respectively. The flexural strength, fracture resistance, and toughness of the composites were substantially higher than those of the results of the nine groups of orthogonal experiments. This occurred because the wheat straw and enzymatic hydrolysis lignin fillers were properly distributed in the matrix, which created good dispersion and compatibility between each other and formed a dense and uniformly stable cross-linked structure. Thus, the composites showed good mechanical properties. The melt index of the composite prepared with the optimum proportion was 2.07 g/10 min, which indicated that the composite had a good processing flow ability.

Bending and Compressive Properties of Composite Pilot-products

According to the authors' previous work on WS/HDPE composites, the optimum ratio of the orthogonal test scheme was selected, and the experimental schemes A and C were used as contrasting schemes. The specific scheme of the composite products is shown in Table 9. Various factors were added to the scheme relative to the content of the matrix polyethylene (HDPE). The wheat straw and enzymatic hydrolysis lignin needed to be dried to control moisture below 5%. The composite pilot-products are presented in Fig. 1.

Table 9. Proportion Schemes of the Composite Pilot-products

Scheme	WS (%)	EHL (%)	CaCO ₃ (%)	MAH-g-PP (%)
A	55	0	5	5
B	50	5	5	5
C	0	55	5	5



Fig. 1. The fractured end surfaces of different composite pilot-products

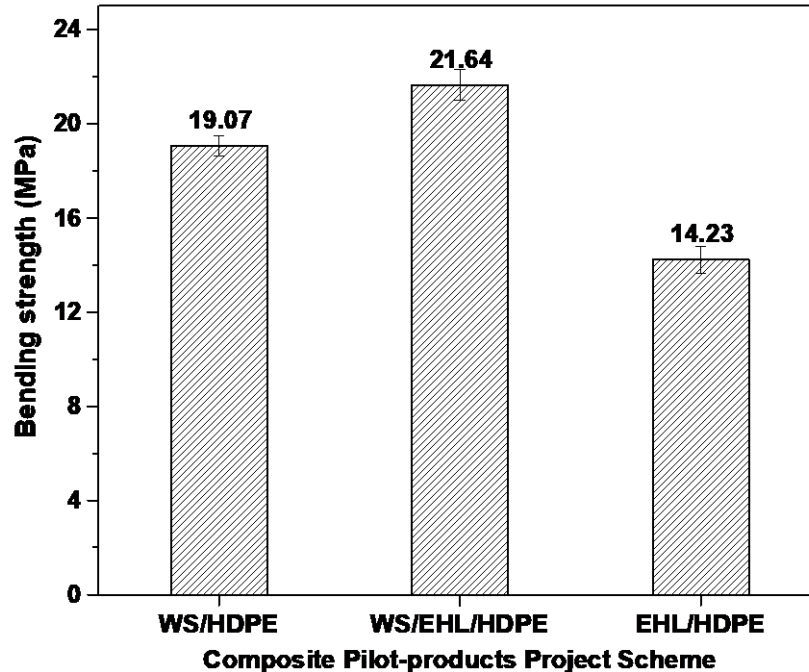


Fig. 2. The bending strength of the composite pilot-products prepared using various schemes

As shown in Fig. 2, the bending strength of the composite pilot product prepared from the WS/EHL/HDPE scheme was 21.6 MPa, which was 11.9% and 34.2% higher than those prepared using the WS/HDPE and EHL/HDPE schemes, respectively. This was because the straw fibers provided a supportive framework in the WS/EHL/HDPE composites similar to that of a “biosteel” structure. The improvement in bending strength that followed the incorporation of EHL to the composites was attributed to the improved dispersibility of the blended system.

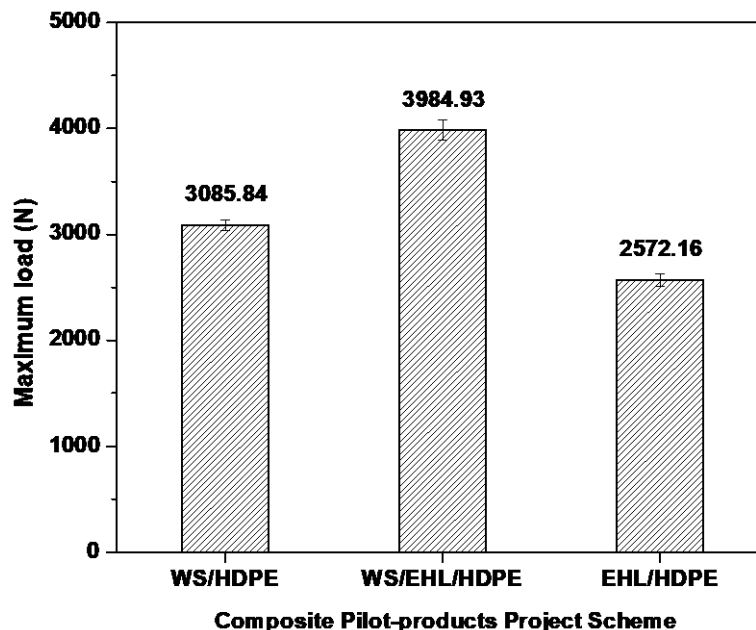


Fig. 3. The maximum load of the composite pilot-products prepared from different schemes

Specifically, when WS blended with the polyethylene matrix forms microstructural gaps, which leads to stress concentration. However, the EHL has a smaller particle size, mostly spherical or flaky, but a larger surface area that could effectively fill the micro-gaps and help to improve the dispersibility of the blended system. The synergistic effect of the fiber component enhanced the interface compatibility of fiber and polymer, and thus the composite showed better mechanical properties. The bending strength of the EHL/HDPE composite was the worst of the three composites due to its excessive amount of lignin, which led to its aggregation in the polymer matrix. The stress concentration of the composite resulted in interstitial defects, so the strength of the composite decreased accordingly.

The maximum load of the WS/EHL/HDPE composite pilot product was 3985 N, as shown in Fig. 3, which was equivalent to a maximum load-bearing capacity of at least 400 kg (calculated with acceleration due to gravity of 9.8 N/kg). As such, its load-bearing capacity was higher than the carrying capacity of both WS/HDPE (3086 N) and EHL/HDPE (2572.16 N), which was consistent with their observed bending performances.

Thermal Stability Analysis of Composites

The thermal degradation of thermoplastic composites is an important reference for their application and aging properties. Thermogravimetric analysis was used to study the thermal degradation behavior of the WS/EHL/HDPE composites, and the thermal stability of the various materials was investigated. Figure 4 is the TGA curve of WS, EHL, HDPE, and the composites in a nitrogen atmosphere with a heating rate of 10 °C/min. Figure 5 is the corresponding first derivative (DTG) curve of the thermogravimetry plot, in which HDPE and WS/HDPE composites were used as contrast samples.

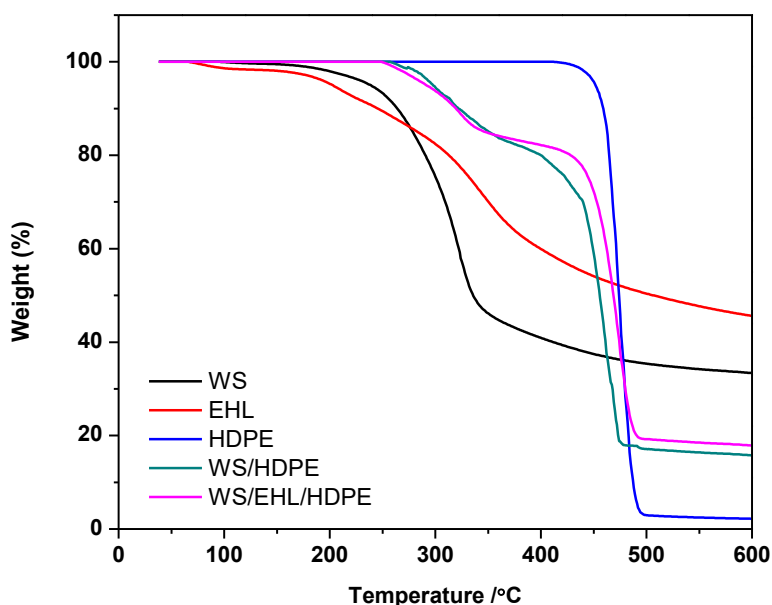


Fig. 4. TGA curves of the raw materials and composites

As shown in Fig. 4, there were two degradation stages in the WS/HDPE composites and the WS/EHL/HDPE composites. In the first stage (temperatures below 400 °C), the first weight loss peak of the composite material was at approximately 323 °C, and the T_{max} values of WS and EHL were 323 °C and 351 °C, respectively. The results showed that this

stage mainly consisted of the thermal degradation of WS and EHL. In the second stage (temperatures over 400 °C), the maximum weight loss peak of the composites was near 474 °C, so this stage mainly corresponded to the thermal degradation of the matrix HDPE. There were two degradation phases in the composites, which were clearly caused by the degradation of the matrix polyethylene after the degradation of WS and EHL.

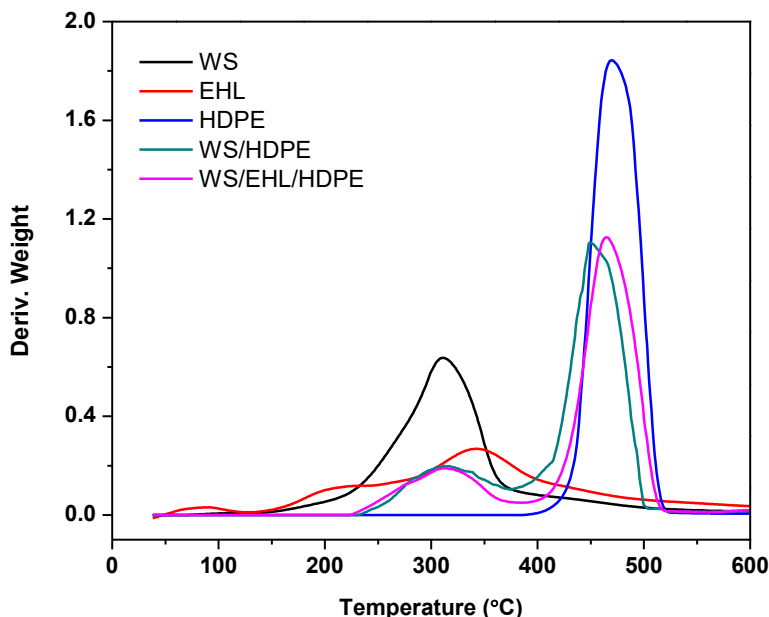


Fig. 5. DTG curves of the raw materials and composites

Figure 5 shows that the maximum weight loss rate of the WS/EHL/HDPE composites tended to shift to the right when compared with the WS/HDPE composites, which indicated that the thermal stability of the composites was improved by adding the enzymatic hydrolysis lignin. The weight loss curves of the wheat straw and enzymatic hydrolysis lignin each had a small weight loss peak at 100 °C, which was attributed to water evaporation. Conversely, the composites did not show remarkable weight loss at this stage, which indicated that the water absorption of the composites decreased. The EHL had a second small weight loss peak at 211 °C, which may have been due to the partial degradation of the lignin into low molecular weight products. With the decrease in molecular weight, the thermal stability of the lignin gradually declined. After 600 °C, the terminal residue represents ash that devoid of all volatile components and remnant lignin. (Yang *et al.* 2007).

FT-IR Analysis of Composites

The infrared spectrum (FT-IR) was used to analyze the chemical structure of the organic polymers and the state of the functional groups. The types of chemical reactions and chemical bonds in the composites can be inferred *via* the intensity and position of the absorption peaks corresponding to the wavenumber. Figure 6 shows the infrared spectra of WS/EHL and their composites.

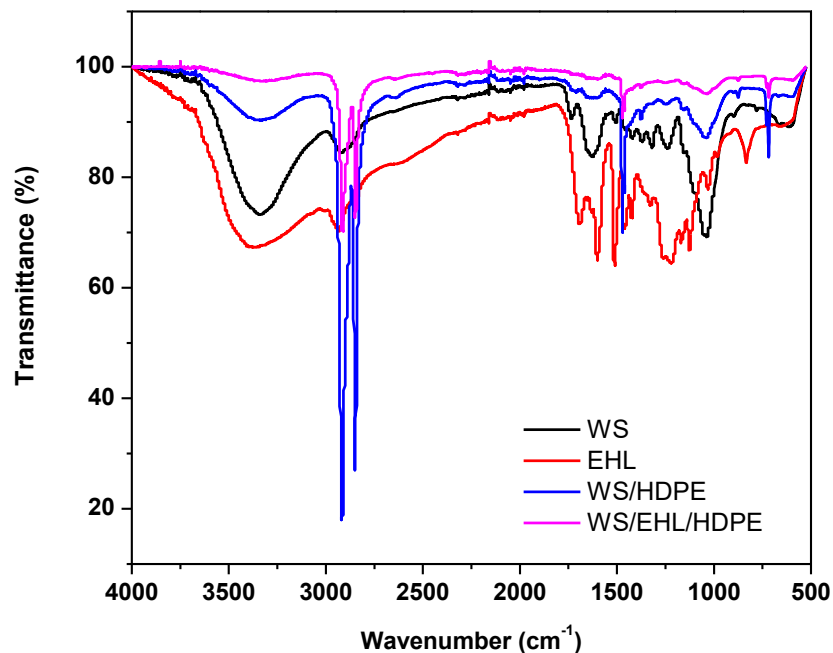


Fig. 6. FTIR spectra of the materials and composites

The FTIR spectra showed that the WS and EHL absorption peaks were relatively broad in the vicinity of 3400 cm^{-1} . This is the characteristic peak of the -OH stretching vibration (Santos *et al.* 2014). This indicated that there were a large number of hydroxyl groups in the fiber raw material that had high polarity and strong hydrophilicity. However, the -OH absorption peak intensity of the composites was weak, which indicated that hydroxyl groups were consumed. In the composite materials, functional groups, such as carboxyl or ester groups, were mainly esterified and condensed with the hydroxyl groups of WS and EHL. This reduction in turn reduced the polarity of the plant fiber and helped to improve the compatibility between the fiber and the nonpolar polyethylene plastic matrix. The absorption peak at around 2900 cm^{-1} to 2800 cm^{-1} is the stretching vibration peak of C-H bonds in saturated alkyl groups, mainly caused by a combination of the molecular structure of the cellulose from wheat straw, the structure of the benzene in the lignin, and the structure of the saturated olefin chains of the polyethylene component in the composites (Sun *et al.* 2014). The C-H absorption peak intensity of the WS/EHL/HDPE composite was weaker than that of the WS/HDPE composite, which showed that the addition of EHL effectively reduced the polar groups of the composites to some extent.

The peak near 1700 cm^{-1} is the stretching vibration of carbonyl C=O moieties, which generally exist in hemicellulose and lignin (Qin *et al.* 2011). However, the absorption peak intensity of this band was clearly weakened in the composites. In particular, the WS/EHL/HDPE composite had almost no absorption peak at this wave number, which indicated that the chemical structure of the composite had changed. Likely due to the good chemical bonding between the fiber and the matrix polyethylene under the action of MAH-g-PP, the interface compatibility between them was improved. These chemical reactions showed that the physical and chemical properties of the composites were improved by the addition of the EHL. The characteristic peaks at 1600 cm^{-1} and 1450 cm^{-1} are very apparent, and they arise mainly because of the vibrations of the benzene ring in the lignin aromatic ring structure and the conjugated olefinic bond of furfural resulting from hemicellulose hydrolysis (Jiang *et al.* 2006).

In the vicinity of 1200 cm^{-1} to 1100 cm^{-1} , the broad and strong characteristic peaks are the complex peaks of various functional groups, mainly attributed to the ester bond (C-O), ether linkage (C-O-C), and other chemical groups in the organic components (Ismail *et al.* 2011). The composite had a sharp absorption peak at 700 cm^{-1} , which arises from the deformation of the outer plane of the aromatic ring that is related to the structure of the benzene ring of lignin in the composites (Pérez *et al.* 2007).

Microstructure of Composites

To investigate the dispersion and interfacial binding of WS and EHL in the polyethylene matrix, SEM was used to observe the fractured surfaces of the composites and fiber raw materials. Figure 7 shows the SEM photomicrographs of wheat straw and enzymatic-hydrolysis lignin. As shown in Fig. 7, the shapes of the two kinds of fiber were more complex and had fragmented and irregular structures. As a "biosteel" in the composite, the wheat straw fiber can support the structure of the composite, which is beneficial to increase the mechanical properties of composites. Meantime, the porous structure of the fiber was also beneficial to interact and cross-link in the matrix polymer to form a multidimensional network structure. Enzymatic-hydrolysis lignin mainly appeared to irregular, flaky, or spherical shape, which was likely attributed to fibers swelling by enzymatic treatment, or the micro-environment changes by weak acid or organic solvent extraction.

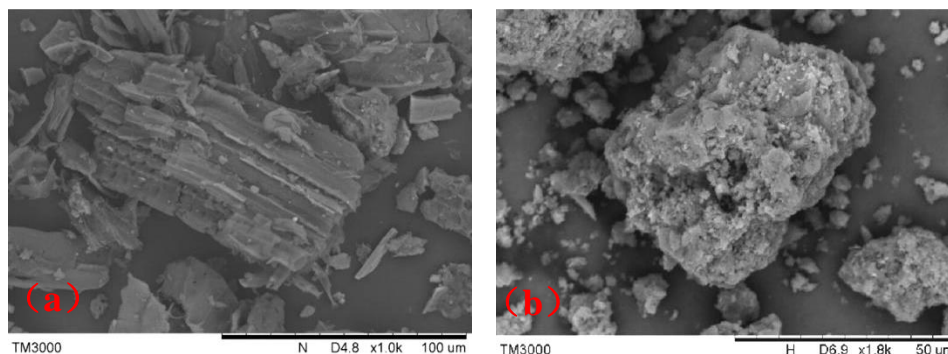


Fig. 7. SEM micrographs of wheat straw (a) and enzymatic-hydrolysis lignin (b)

Figure 8 shows the scanning electron micrographs of the fractured surfaces of the two composites. It can be seen from Fig. 8(c & d) that for WS/EHL, the dispersion of the fillers in the polyethylene matrix was more uniform, and there was no reunion phenomenon. This indicated that the WS, EHL, and other fillers, which was treated by mechanical shearing in the two-spindled mechanical mixer, had viable dispersion effects in HDPE matrix during the processing. Furthermore, from the perspective of the two phase interface, the combination of WS/EHL and polyethylene was more compact than that of the WS/HDPE composites, and a mutual compatibility structure was formed that helped the composite material to exhibit better physical and mechanical properties. In Fig. 8(a & b), voids in the fractured surface of the composite were clearly visible, which indicated the poor bonding between the fibers and the matrix. This was consistent with the other test results under optimal conditions.

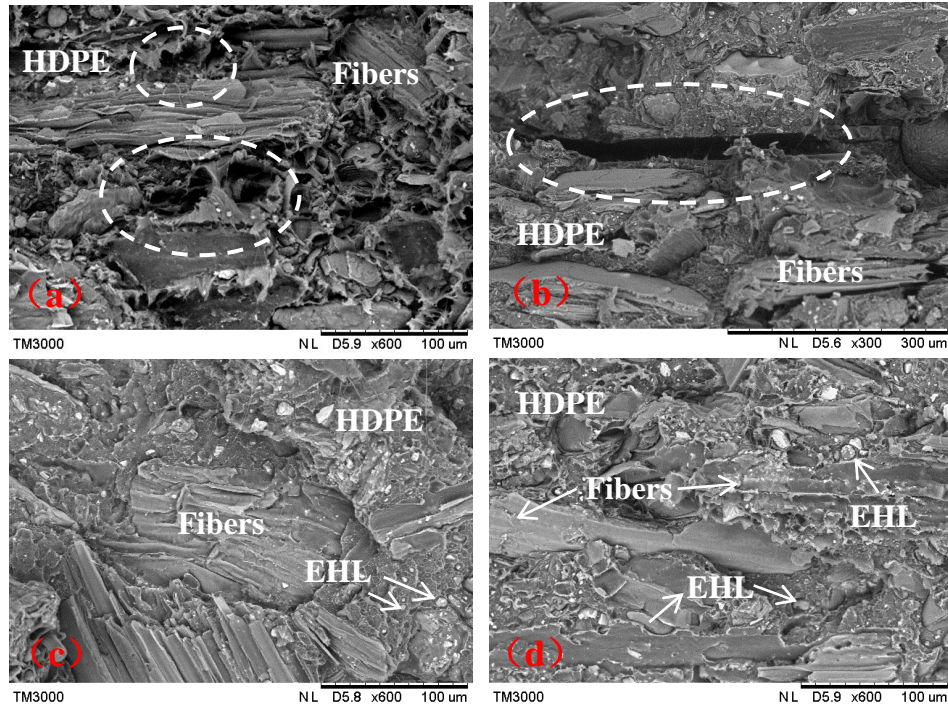


Fig. 8. SEM micrographs of WS/HDPE composites (a & b) and WS/EHL/HDPE composites (c & d)

Based on the above mentioned WS/HDPE composites' structural model (Fig. 9a), the novel WS/EHL/polyethylene three-dimensional melt blending system was proposed (Fig. 9b).

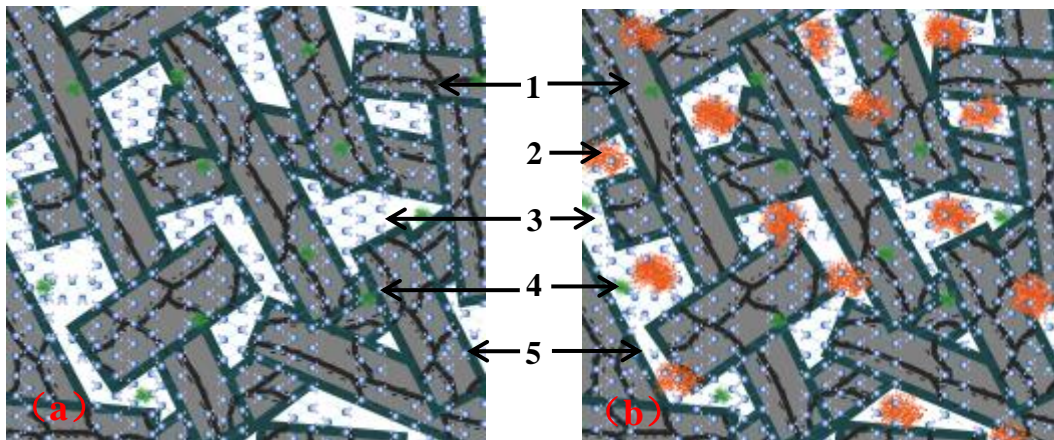


Fig. 9. A schematic illustration of the structural model of WS/HDPE composites (a) and WS/EHL/HDPE composites (b); 1: wheat straw fibers; 2: EHL; 3: HDPE polymer; 4: CaCO_3 ; and 5: MAH-g-PP

In this model, the wheat straw fibers (1) were uniformly filled in the polymer matrix (3) and played the role of “biosteel”. The structural properties of the enzymatic hydrolysis lignin (2) were helpful for the inclusion and attachment of polymers, improving the dispersibility in the matrix and contributing to the formation of a dense, more homogeneous composite structure. CaCO_3 (4) not only fills the porous network structure of wheat straw

by mechanical agitation, increases fiber bulk density, but also displays toughening effects and improves impact strength of the composite. MAH-g-PP (5) provided better chemical bonding between fibers and polymers and improved the compatibility and processability of the composites. The model reflected the relevant properties and advantages of the WS/EHL/HDPE composites and their corresponding pilot products accordingly.

CONCLUSIONS

1. The optimal ratio of WS, EHL, CaCO₃, and MAH-g-PP in the composites was 50%, 5%, 5%, and 5%, respectively, which was determined through orthogonal experiments. Composites prepared with the optimum proportions showed improved flexural strength (42.2 MPa), tensile strength (19.9 MPa), impact strength (4.12 KJ/m²), and melt index (2.07 g/10 min), which resulted in improved mechanical properties and processing fluidity.
2. The composite pilot-product (WS/EHL/HDPE) was found to have a flexural strength of 21.64 MPa and a maximum load bearing capacity of 3985 N, confirming that the mechanical performance of the composite was substantially enhanced compared to composites without EHL.
3. The TGA analysis of the fibers and composites revealed that addition of enzymatic hydrolysis lignin substantially improved the degradation temperature of the WS/EHL/HDPE composite compared to the WS/HDPE composite. The FT-IR analysis and SEM micrographs clearly demonstrated that the polar groups of the fiber components in the composites were “consumed” and that the fibers exhibited good chemical bonding with the matrix polyethylene. Both WS and EHL were well dispersed in the composites, which were closely packed and formed interconnected, interspersed network structures.
4. The use of EHL substantially improved the mechanical performance properties of the newly developed thermoplastic composites and improved the compatibility and dispersion of the fiber components within the matrix polyethylene. Therefore, the use of EHL in composites represents an excellent additional application of the material.

ACKNOWLEDGMENTS

The authors gratefully acknowledge the financial support of the National Key Technology Support Program, the Ministry of Science and Technology, China (2012BAC17B00), the bidding project of Zunyi Medical University (No. F-803), and the Jiangsu Synergetic Innovation Center for Advanced Bio-Manufacture.

REFERENCES CITED

- Alexy, P., Crkonová, G., Gregorová, A., Kosíková, B., and Martis P. (2004).
“Modification of lignin-polyethylene blends with high lignin content using ethylene-

- vinylacetate copolymer as modifier,” *Journal of Applied Polymer Science* 94(5), 1855-1860. DOI: 10.1002/app.20716
- ASTM D256 (2010). “Standard test methods for determining the Izod pendulum impact resistance of plastics,” ASTM International, West Conshohocken, PA.
- ASTM D638 (2010). “Standard test method for tensile properties of plastics,” ASTM International, West Conshohocken, PA.
- ASTM D790 (2010). “Standard test methods for flexural properties of unreinforced and reinforced plastics and electrical insulating materials,” ASTM International, West Conshohocken, PA.
- ASTM D1238 (2013). “Standard test method for melt flow rates of thermoplastics by extrusion plastometer,” ASTM International, West Conshohocken, PA.
- ASTM D6109 (2010). “Standard test methods for flexural properties of unreinforced and reinforced plastic lumber and related products,” ASTM International, West Conshohocken, PA.
- Bekele, L. D., Zhang W. T., Liu Y. L., Duns G. J., Yu C. H., Jin L. L., Li. X. F., Jia Q., and Chen J. S. (2017). “Preparation and characterization of lemongrass fiber (*Cymbopogon* species) for reinforcing application in thermoplastic composites,” *BioResources* 12(3), 5664-5681. DOI: 10.15376/biores.12.3.5664-5681
- Canetti, M., Bertini, F., Chirico, A. D., and Audisio, G. (2006). “Thermal degradation behaviour of isotactic polypropylene blended with lignin,” *Polymer Degradation and Stability* 91(3), 494-498. DOI: 10.1016/j.polymdegradstab.2005.01.052
- Cazacu, G., Pascu, M. C., Profire, L., Kowarski, A. I., Mihaes, M., and Vasile, C. (2004). “Lignin role in a complex polyolefin blend,” *Industrial Crops and Products* 20(2), 261-273. DOI: 10.1016/j.indcrop.2004.04.030
- Deng, Z. Z., and Zhao, M. (2016). “The optimization of agent formula by orthogonal experiment,” *Procedia Engineering* 135, 649-654. DOI: 10.1016/j.proeng.2016.01.132
- Feldman, D., Banu, D., and El-Aghoury, A. (2007). “Plasticization effect of lignin in some highly filled vinyl formulation,” *Journal of Vinyl and Additive Technology* 13(1), 14-21. DOI: 10.1002/vnl.20098
- Gregorová, A., Cibulková, Z., Košíková, B., and Šimon, P. (2005). “Stabilization effect of lignin in polypropylene and recycled polypropylene,” *Polymer Degradation and Stability* 89(3), 553-558. DOI: 10.1016/j.polymdegradstab.2005.02.007
- Han, G. P., Deng, J., Zhang, S. Y., Bicho, P., and Wu, Q. L. (2010). “Effect of steam explosion treatment on characteristics of wheat straw,” *Industrial Crops and Products* 31(1), 28-33. DOI: 10.1016/j.indcrop.2009.08.003
- Ismail, H., Abdullah, A. H., and Bakar, A. (2011). “Influence of acetylation on the tensile properties, water absorption, and thermal stability of (high-density polyethylene)/(soya powder)/(kenaf core) composites,” *Journal of Vinyl and Additive Technology* 17(2), 132-137. DOI: 10.1002/vnl.20262
- Jiang, Z. H., Yu, W. J., and Yu, Y. L. (2006). “Analysis of chemical components of bamboo wood and characteristics of surface performance,” *Journal of Northeast Forestry University* 34(4), 1-2, 6.
- Kosikova, B., and Gregorova, A. (2005). “Sulfur-free lignin as reinforcing component of styrene-butadiene rubber,” *Journal of Applied Polymer Science* 97(3), 924-929. DOI: 10.1002/app.21448

- Liany, Y., Tabei, A., Farsi, M., and Madanipour, M. (2013). "Effect of nanoclay and magnesium hydroxide on some properties of HDPE/wheat straw composites," *Fibers and Polymers* 14(2), 304-310. DOI: 10.1007/s12221-013-0304-3
- Maneesh, T., Singh, V. K., Gope, P. C., and Chaudhary, A. K. (2012). "Evaluation of mechanical properties of bagasse-glass fiber reinforced composite," *J. Mater. Environ. Sci.* 3 (1), 171-184.
- Matuana, L. M., and Stark, N. M. (2003). "Ultraviolet weathering of photostabilized wood-flour-filled high-density polyethylene composites," *Journal of Applied Polymer Science* 90(10), 2609-2617. DOI: 10.1002/app.12886
- Mengeloglu, F., Kurt, R., Gardner, D. J., and O'Neill, S. (2007). "Mechanical properties of extruded high density polyethylene and polypropylene wood flour decking boards," *Iran. Polym. J.* 16 (7), 477-487.
- Panthapulakkal, S., Zereshkian, A., and Sain, M. (2006). "Preparation and characterization of wheat straw fibers for reinforcing application in injection molded thermoplastic composites," *Bioresource Technology* 97(2), 265-272. DOI: 10.1016/j.biortech.2005.02.043
- Pérez, J. M., Rodríguez, F., Alonso, M. V., Oliet, M., and Echeverría, J. M. (2007). "Characterization of a novolac resin substituting phenol by ammonium lignosulfonate as filler or extender," *BioResources* 2(2), 270-283. DOI: 10.15376/biores.2.2.270-283
- Pucciariello, R., Villani, V., Bonini, C., D'Auria, M., and Vetere, T. (2004). "Physical properties of straw lignin-based polymer blends," *Polymer* 45(12), 4159-4169. DOI: 10.1016/j.polymer.2004.03.098
- Qin, L. J., Qiu, J. H., Liu, M. Z., Ding, S. L., Shao, L., Lü, S., Zhang, G. H., Zhao, Y., and Fu, X. (2011). "Mechanical and thermal properties of poly(lactic acid) composites with rice straw fiber modified by poly(butyl acrylate)," *Chemical Engineering Journal* 166(2), 772-778. DOI: 10.1016/j.cej.2010.11.039
- Rangaraj, S. V., and Smith, L. V. (2000). "Effects of moisture on the durability of a wood/thermoplastic composite," *Journal of Thermoplastic Composite Materials* 13(2), 140-161. DOI: 10.1106/5NV3-X974-JDR1-QTAL
- Rodrigues, P. C., Cantao, M. P., Janissek, P., Scarpa, P. C. N., Mathias, A. L., Ramos, L. P., and Gomes, M. A. B. (2002). "Polyaniline/lignin blends: FTIR, MEV and electrochemical characterization," *European Polymer Journal* 38(11), 2213-2217. DOI: 10.1016/S0014-3057(02)00114-3
- Santos, P. S. B., Erdocia, X., Gatto, A. D., and Labidi, J. (2014). "Characterisation of kraft lignin separated by gradient acid precipitation," *Industrial Crops and Products* 55, 149-154. DOI: 10.1016/j.indcrop.2014.01.023
- Selke, S. E., and Wichman, I. (2004). "Wood fiber/polyolefin composites," *Composites Part A: Applied Science and Manufacturing* 35(3), 321-326. DOI: 10.1016/j.compositesa.2003.09.010
- Sirapat, C., Sirijutaratana, C., and Petchwattana, N. (2012). "Mechanical properties, thermal degradation and natural weathering of high density polyethylene/rice hull composites compatibilized with maleic anhydride grafted polyethylene," *J. Polym. Res.* 19(7), 1-10.
- Sun, S. L., Wen, J. L., Ma, M. G., Sun, R. C., and Jones, G. L. (2014). "Structural features and antioxidant activities of degraded lignins from steam exploded bamboo stem," *Industrial Crops and Products* 56, 128-136. DOI: 10.1016/j.indcrop.2014.02.031

- Toress, F. G., and Cubillas, M. L. (2005). "Study of the interfacial properties of natural fiber reinforced polyethylene," *Polym. Test.* 24, 694-698. DOI: 10.1016/j.polymertesting.2005.05.004
- Wambua, P., Iven, J., and Verpoest, I. (2003). "Natural fibers: Can they replace glass fiber reinforced plastics?" *Compos. Sci. Technol.* 63, 1259-1264. DOI: 10.1016/S0266-3538(03)00096-4
- Wang, W. H., Wang, Q. W., and Zhang, Z. M. (2008). "Natural weathering and accelerated UV weathering of rice-hull-polyethylene composite," *Scientia Silvae Sinicae* 44(8), 90-94.
- Xiao, B., Sun, X. F., and Sun, R. C. (2001). "The chemical modification of lignins with succinic anhydride in aqueous systems," *Polymer Degradation and Stability* 71(2), 223-231. DOI: 10.1016/S0141-3910(00)00133-6
- Yang, H., Yan, R., Chen, H., Lee, D. H., and Zheng, C. (2007). "Characteristics of hemicellulose, cellulose and lignin pyrolysis," *Fuel* 86, 1781-1788. DOI: 10.1016/j.fuel.2006.12.013
- Zhang, W. T., Chen, J. S., Bekele, L. D., Liu, Y. L., Duns, G. J., and Jin, L. L. (2016). "Physical and mechanical properties of modified wheat straw filled polyethylene composites," *BioResources* 11(2), 4472-4484. DOI: 10.15376/biores.11.2.4472-4484
- Zou, Y., Huda, S., and Yang, Y. (2010). "Lightweight composites from long wheat straw and polypropylene web," *Bioresource Technology* 101(6), 2026-2033. DOI: 10.1016/j.biortech.2009.10.042

Article submitted: December 22, 2017; Peer review completed: February 17, 2018;
Revised version received and accepted: March 8, 2018; Published: March 14, 2018.
DOI: 10.15376/biores.13.2.3219-3235